Modelling of aluminium sheet material at elevated temperatures

L. van Haaren[1], A.H. van den Boogaard[2], J. Huétink[2]

[1]*Netherlands Institute for Metals Research, P.O. Box 5008, 2600 GA Delft, Netherlands*
URL: www.nimr.nl *e-mail: l.vanhaaren@ctw.utwente.nl*

[2]*Faculty of Engineering Technology, University of Twente, P.O. Box 217, 7500 AE Enschede, Netherlands*
URL: www.tm.ctw.utwente.nl *e-mail: a.h.vandenboogaard@ctw.utwente.nl; j.huetink@ctw.utwente.nl*

ABSTRACT: The formability of Al–Mg sheet can be improved considerably, by increasing the temperature. At elevated temperatures, the mechanical response of the material becomes strain rate dependent. To accurately simulate warm forming of aluminium sheet, a material model is required that incorporates the temperature and strain-rate dependency. In this paper hardening is described succesfully with a physically based material model for temperatures up to 200 °C. At higher temperatures and very low strain rates, the flow curve deviates significantly from the model. Strain rate jumps still pose a serious problem to the models.

Key words: aluminium, warm forming, hardening, modelling

1 INTRODUCTION

In deep drawing of a cylindrical aluminium cup, the limiting drawing ratio can be increased considerably by controlling the temperature of different parts of the sheet. By heating the flange up to 250 °C and cooling the punch the limiting drawing ratio could be increased from 2.1 to 2.6 for a 5754-O alloy [1, 2]. The optimal temperature distribution and punch velocity depend on the type of aluminium and the tool geometry. Because experience is lacking, computational analysis can assist in determination of the process window.
For a proper simulation of the warm forming process a sufficiently accurate material model is needed. For the plastic deformation of aluminium at elevated temperatures, the most important property is the hardening model, including temperature and strain rate dependency. Some possible hardening models are described in this paper.

2 HARDENING MODEL

The flow stress σ_f is a measure for the resistance to (further) plastic deformation of a material. Experiments show that the work hardening in Al–Mg alloys depends on the deformation, temperature and strain rate.
For numerical analysis, a description of this work hardening is needed. The classical approach is to fit macroscopic mechanical measurements to a convenient mathematical function. The validity of these phenomenological models is limited to situations that are comparable to the range of experiments on which they are based. Models that are based on the physics of plastic deformation may have a wider applicability.

2.1 The Extended Nadai Model

A typical phenomenological model is the Nadai or Swift relation. To add strain rate sensitivity to this relation, a power law is used:

$$\sigma_\mathrm{f} = C(\varepsilon + \varepsilon_0)^n \dot{\varepsilon}^m \tag{1}$$

To incorporate temperature dependency, the parameters C, n and m can be made temperature dependent as demonstrated in [1].

2.2 The Bergström Model

The physically based model used here starts with a decomposition of the flow stress into a strain and strain rate independent stress σ_0, a dynamic stress σ^* that depends on the strain rate and temperature and a term σ_w that incorporates the work hardening:

$$\sigma_\mathrm{f} = \sigma_0(T) + \sigma^*(\dot{\varepsilon}, T) + \sigma_\mathrm{w}(\rho, T) \tag{2}$$

In simulation programs, the dynamic stress σ^* is often defined by

$$\sigma^*(\dot{\varepsilon}, T) = \sigma_0^* \left(1 + \frac{kT}{\Delta G_0} \ln \frac{\dot{\varepsilon}}{\dot{\varepsilon}_0}\right)^p \tag{3}$$

limited between 0 for small strain rates and σ_0^* for $\dot{\varepsilon} > \dot{\varepsilon}_0$. This relation is based on a probabilistic approach in statistical thermodynamics. The physical background suggests that p should not differ too much from 1.

In experimental stress–strain curves it is observed that the influence of the strain rate on the initial yield stress is small between 300 K and 450 K and increases rapidly between 450 K and 525 K. In the whole temperature range, Equation (3) shows a large strain rate influence at low temperatures that vanishes at high temperatures. This is in contradiction with the observations and therefore the dynamic stress σ^* is neglected altogether for the investigated Al–Mg alloy.

The work hardening part of the model, σ_w, takes the evolution of the micro-structure into account. A relatively simple one-parameter model is used, where the evolution of the dislocation density ρ is responsible for the hardening. The relation between the dislocation density and σ_w is given by the Taylor equation:

$$\sigma_\mathrm{w} = \alpha G(T) b \sqrt{\rho} \tag{4}$$

where α is a scaling parameter of order 1.

The essential part in these models is the evolution of the dislocation density ρ. The creation and storage of dislocations is taken to be proportional to the mean free path, while dynamic recovery is taken to be proportional to the dislocation density itself. This leads to the basic equation for the Bergström model [3] as well as the family of Kocks–Mecking models:

$$\frac{\mathrm{d}\rho}{\mathrm{d}\varepsilon} = c_1 \frac{1}{L} - c_2 \rho \tag{5}$$

where the recovery parameter c_2 depends on temperature and strain rate.

In the original Bergström model, the mean free path L was considered to be constant. The formation of dislocation walls and the principle of similitude led Vetter and van den Beukel [4], to a storage factor that is proportional to the square root of the dislocation density. The dynamic recovery term is considered to be due to annihilation and remobilisation of immobile dislocations. The remobilisation is a thermally activated process, based on vacancy climb [5]. The evolution of dislocation density is then reformulated as

$$\frac{\mathrm{d}\rho}{\mathrm{d}\varepsilon} = U(\rho) - \Omega(\dot{\varepsilon}, T)\rho \tag{6a}$$

with

$$U = U_0 \sqrt{\rho} \tag{6b}$$

$$\Omega = \Omega_0 + C \exp\left(-\frac{m Q_\mathrm{v}}{RT}\right) \dot{\varepsilon}^{-m} \tag{6c}$$

The function U represents storage of mobile dislocations (immobilisation), and Ω represents dynamic recovery by remobilisation and annihilation. The functions U and especially Ω determine the shape of the hardening curve at different temperatures and strain rates. Q_v is an activation energy for vacancy migration.

Equation (6a) can be integrated analytically for constant U_0 and Ω. For an incremental algorithm the dislocation density ρ_{i+1} at time t_{i+1} can be calculated from

$$\rho_{i+1} = \left[\frac{U_0}{\Omega}\left(\exp\frac{\Omega\Delta\varepsilon}{2} - 1\right) + \sqrt{\rho_i}\right]^2 \exp(-\Omega\Delta\varepsilon) \tag{7}$$

For constant temperature and strain rate, substitution of (7) into (4) yields the Voce hardening equation. For non-constant temperature or strain rate, the two models differ. The Voce relation will result in an immediate stress change on a strain rate or temperature change, while the Bergström model is actually an evolution equation and, accordingly, the stress will only change gradually.

Finally the strain rate independent stress $\sigma_0(T)$ from Equation (2) must be determined. It is assumed that this stress is related to stresses in the atomic lattice. Hence, the temperature dependence of the shear modulus $G(T)$ is also used for σ_0. The flow stress is now evaluated by

$$\sigma_\mathrm{f} = g(T)\left(\sigma_0 + \alpha G_\mathrm{ref} b \sqrt{\rho}\right) \tag{8}$$

where $g(T)$ is the shear modulus divided by the reference value G_ref. The temperature dependence is numerically represented in this work by the empirical relation

$$g(T) = 1 - C_\mathrm{T} \exp\left(-\frac{T_1}{T}\right) \tag{9}$$

where C_T and T_1 are fitting parameters.

2.3 Comparison with Experiments

Some of the parameters in the Bergström model can be selected beforehand. The rest is determined by a least squares approximation of experimental results.

The initial dislocation density ρ_0, the magnitude of the Burgers vector b and the shear modulus at room

Table 1: Parameters for the Bergström model.

σ_0	109.3 MPa	m	0.422
α	1.0	U_0	$6.093 \cdot 10^8\,\mathrm{m}^{-1}$
b	$2.857 \cdot 10^{-10}\,\mathrm{m}$	Ω_0	23.63
C	$3.3422 \cdot 10^5$	Q_v	$1.0917 \cdot 10^5\,\mathrm{J/mol}$
ρ_0	$10^{11}\,\mathrm{m}^{-2}$	G_ref	26354 MPa
C_T	38.45	T_1	2975 K

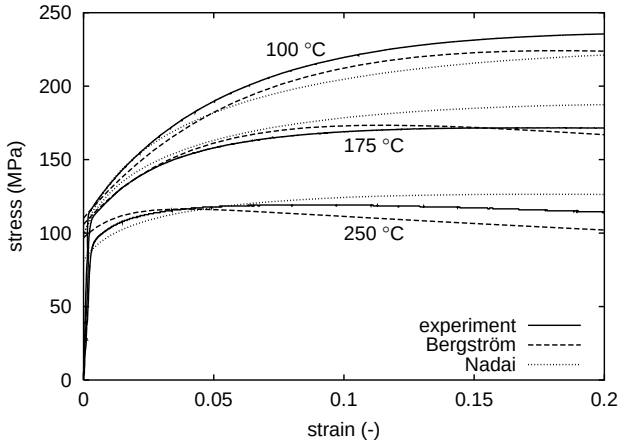

(a) $\dot{\varepsilon} = 0.002\,\mathrm{s}^{-1}$

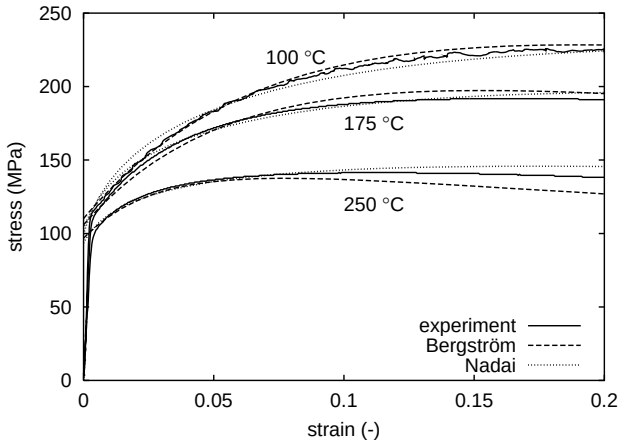

(b) $\dot{\varepsilon} = 0.02\,\mathrm{s}^{-1}$

Figure 1: Engineering stress–strain curves — experiments and models.

temperature G_ref were taken from the literature and a value of $\alpha = 1.0$ was chosen. The parameters C_T and T_1 could have been fitted to experimental values of the shear modulus, but better results were obtained by fitting them to the hardening curves, simultaneously with the other parameters.

The remaining parameters were fitted to 8 tensile tests at 4 different temperatures and 2 different strain rates. It resulted in the values presented in Table 1.

In Figure 1 the simulated engineering stress–strain curves are plotted for the extended Nadai model and the Bergström model, together with the experimental data. It can be seen that both models are more or less capable of describing the experiments. It should be noted that the comparison is only valid for a uniform strain, which means up to the maximum engineering stress.

At room temperature (not presented), the experiments and both models almost coincide. The stress–strain curves for temperatures of 100 °C, 175 °C and 250 °C are plotted in Figure 1(a) for a strain rate of $0.002\,\mathrm{s}^{-1}$ and in Figure 1(b) for a strain rate of $0.02\,\mathrm{s}^{-1}$. For the higher strain rate, both models perform quite well. For the lower strain rate the differences are larger. The Bergström model does not perform very well if the initial yield stress is overestimated as in the low strain rate case at 250 °C.

2.4 Strain Rate Jumps

Each curve in Figure 1 was obtained at constant temperature and constant strain rate. If the temperature or strain rate is changed during deformation, it is not obvious that the stress will immediately adapt to the new situation. The evolution of micro-structure during deformation may depend on the strain rate and at a sudden increase in strain rate, the micro-structure is still determined by the initial lower strain rate.

Experiments with strain rate jumps are presented in Figure 2(a). It can be observed that the stress increased very rapidly after increasing the strain rate from $0.002\,\mathrm{s}^{-1}$ to $0.02\,\mathrm{s}^{-1}$ and then increased further at a lower rate until the curve was reached that represents the test with a constant strain rate of $0.02\,\mathrm{s}^{-1}$. The direct influence seems to be larger for the 250 °C experiment than for the 175 °C experiment. For a decreasing strain rate, the direct influence on the stress was much larger. In the 250 °C experiment, the stress dropped immediately to the lower strain rate curve and no transient phenomenon was observed.

Although the models yield more or less similar stress–strain curves for constant strain rate simulations, the predictions are completely different if a jump in the strain rate is simulated. In Figure 2 the stress–strain curves are plotted for deformation at 175 °C and 250 °C and for strain rates of $0.002\,\mathrm{s}^{-1}$ and $0.02\,\mathrm{s}^{-1}$. If strain rate changes from $0.002\,\mathrm{s}^{-1}$ to $0.02\,\mathrm{s}^{-1}$ or from $0.02\,\mathrm{s}^{-1}$ to $0.002\,\mathrm{s}^{-1}$ are applied after a strain of 5 %, the Nadai model immediately follows the curve corresponding to a constant strain rate. With the Bergström model the constant strain rate curve is only slowly approached after continuous straining. These predictions should be compared with the experiments as presented in Figure 2(a). It shows that real material behaviour is somewhere in between and should be investigated more thoroughly.

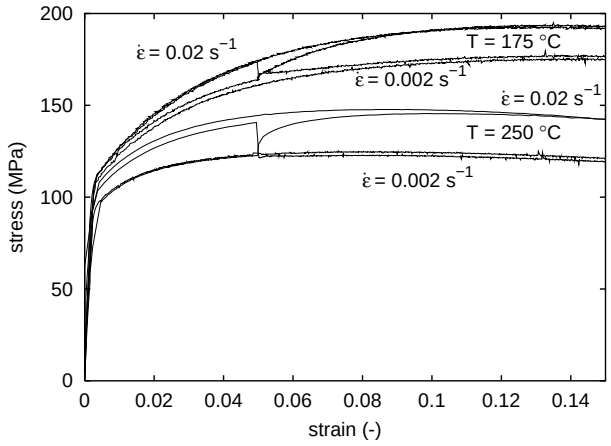

(a) Experiments

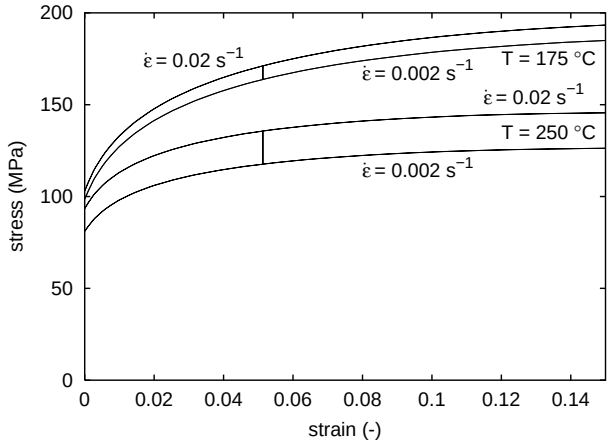

(b) extended Nadai model

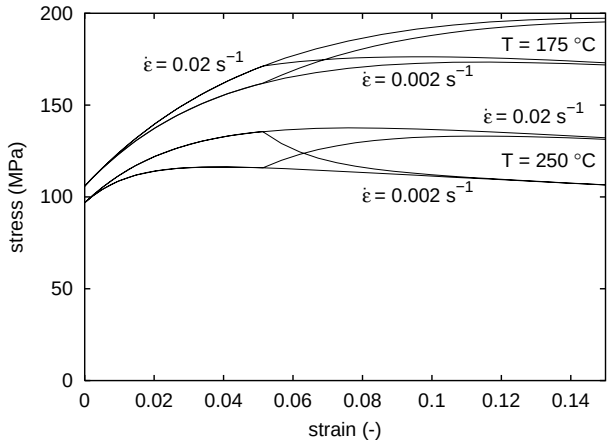

(c) Bergström model

Figure 2: Engineering stress–strain curves with and without strain rate jumps at 250°C.

3 DISCUSSION

The work hardening at different temperatures and strain rates was modelled by adapting the parameters of a Nadai model and with a Bergström model. The temperature and strain rate sensitivity enters the Bergström model through a relatively simple modelling of dynamic recovery. It can predict stress–strain curves at constant strain rate very well, apart from high-temperature/low-strain-rate situations. The response on strain rate jumps is too slow. More recent physically based models are extensions of the one-parameter models. Nes [6] distinguished dislocation densities in cell walls and in cell interiors, considering the sub-grain size δ and misorientation ϕ he models the critical shear stress as:

$$\tau = \tau_i + \alpha_1 Gb\sqrt{\rho_i} + \alpha_2 Gb\frac{1}{\delta} \tag{10}$$

The presented results are good, but the experimental validation seems to be focused on rolling of aluminium at higher temperatures than in warm forming. Different evolution equations for ρ_i and δ are used during the phase II, phase III and phase IV stages of hardening. This may improve the agreement of model and experiments for the high-temperature/low-strain-rate situation and the strain rate jumps. Advanced models like this one are currently under investigation for their applicability to warm forming.

ACKNOWLEDGEMENTS

This research was carried out under projectnumber MC1.02106 in the framework of the Strategic Research programme of the Netherlands Institute for Metals Research in the Netherlands (www.nimr.nl).

REFERENCES

[1] A. H. van den Boogaard, P. J. Bolt, and R. J. Werkhoven. Modeling of AlMg sheet forming at elevated temperatures. *International Journal of Forming Processes*, 4:361–375, 2001.

[2] A. H. van den Boogaard. *Thermally enhanced forming of aluminium sheet—Modelling and experiments*. PhD thesis, University of Twente, 2002.

[3] Y. Bergström. Dislocation model for the stress-strain behaviour of polycrystalline α-Fe with special emphasis on the variation of the densities of mobile and immobile dislocations. *Materials Science and Engineering*, 5:193–200, 1969.

[4] R. Vetter and A. van den Beukel. Dislocation production in cold worked copper. *Scripta Metallurgica*, 11: 143–146, 1977.

[5] Y. Bergström. The plastic deformation of metals—a dislocation model and its applicability. *Reviews on Powder Metallurgy and Physical Ceramics*, 2:105–115, 1983.

[6] E. Nes. Modelling of work hardening and stress saturation in FCC metals. *Progress in Materials Science*, 41:129–193, 1998.